A Structural, Kinetic Model of Soft Tissue Thermomechanics

Triantafyllos Stylianopoulos,* Alptekin Aksan,† and Victor H. Barocas‡
*Department of Chemical Engineering and Materials Science, †Department of Mechanical Engineering, and ‡Department of Biomedical Engineering, University of Minnesota, Minneapolis, Minnesota

ABSTRACT A structure-based kinetic model was developed to predict the thermomechanical response of collagenous soft tissues. The collagen fibril was represented as an ensemble of molecular arrays with cross-links connecting the collagen molecules within the same array. A two-state kinetic model for protein folding was employed to represent the native and the denatured states of the collagen molecule. The Monte Carlo method was used to determine the state of the collagen molecule when subjected to thermal and mechanical loads. The model predictions were compared to existing experimental data for New Zealand white rabbit patellar tendons. The model predictions for one-dimensional tissue shrinkage and the corresponding mechanical property degradation agreed well with the experimental data, showing that the gross tissue behavior is dictated by molecular-level phenomena.

INTRODUCTION

Subablative heating of collagenous soft tissue is central to therapies such as thermal capsulorraphy (1,2), thermal treatment of the anterior cruciate ligament, knee and elbow laxity (3), thermokeratoplasty (4), treatment of spider veins, saphenous vein closure, and facial cutaneous disorders (skin resurfacing, and port wire stain treatment (5)). These therapies utilize heat-induced denaturation of the collagen molecule, which is the major component of most soft tissues. Depending on the tissue type, hydration level and tensile force on the tissue, collagen denaturation starts in the temperature range 55–75°C. During denaturation, hydrogen bonds that stabilize the triple-helical structure of the collagen molecule break, and the molecule unfolds irreversibly from its native state (6,7). Even though there is an increase in the range and popularity of thermal therapies, for many of them there still are no established guidelines for clinical use (7,8). This is mainly attributed to the lack of understanding of the tissue response.

At the single-molecule level, collagen denaturation is considered to be an irreversible rate process, governed by first-order kinetics (6,9–11). Thermodynamics of the denaturation process have been widely studied, and values for activation energies and rate constants for many species and tissue types have been reported (10,12). At the tissue level, the outcome of collagen denaturation is observed as shrinkage of the tissue, loss of birefringence, and changes in gross mechanical properties (13–17). There are relatively few published theoretical studies describing the heat-induced alterations in soft tissues. These studies are based either on phenomenological equations (18–20) or on ideas derived from continuum mechanics and classical thermodynamics (21), and do not incorporate molecular-level phenomena to describe the tissue-level behavior.

In this work, a novel methodology for studying the kinetics of thermal denaturation of collagenous tissues is presented and used to predict the thermomechanical response of a homogeneous collagenous tissue composed of a parallel array of fibers. The modeling approach takes into account the microstructure of the tissue and utilizes information at the single-molecule level to obtain the macroscopic response. The predictions of the model are compared to experimental data presented in a previous study (13).

METHODS

Molecular-level modeling

The collagen molecule has a triple-helical structure, where the helices are linked to each other and stabilized by hydrogen bonds. At sufficiently high temperatures, the hydrogen bonds break, resulting in denaturation and shrinkage of the molecule (Fig. 1 *A*). In this research, collagen denaturation is modeled according to two main assumptions:

1. Collagen denaturation at the molecular level is governed by an irreversible rate process and follows first-order kinetics (6,9–11). Therefore, the rate constant can be calculated by the Arrhenius equation.
2. The two-state model of protein folding describes collagen denaturation. According to this model, the collagen molecule has only two configurations, native and denatured. The two-state model implies a stochastic process, making it suitable for the application of the the Monte Carlo method (22,23).

A two-state Gibbs free-energy diagram is shown in Fig. 1 *B* (see also (12)). The native state corresponds to the folded (triple-helical) state of the collagen molecule, and it is thermodynamically favorable at physiological temperatures. With increasing temperature, the collagen molecule gains enough energy to overcome the energy barrier and transitions into the denatured state. Under stress-free conditions, the energy required for the molecule to reach the transition state (i.e., activation Gibbs free energy) is ΔG^{o}.

Assuming irreversible, first-order kinetics, the equation governing the thermal denaturation of a collagen fiber consisting of N collagen molecules in the native state is

Submitted April 27, 2007, and accepted for publication August 17, 2007.

Address reprint requests to Victor H. Barocas, 7-105 Hasselmo Hall, 312 Church St. SE, University of Minnesota, Minneapolis, MN 55455. Tel.: 612-626-5572; Fax: 612-626-6583; E-mail: baroc001@umn.edu.

Editor: Kathleen B. Hall.

0006-3495/08/02/717/09 $2.00

doi: 10.1529/biophysj.107.111716

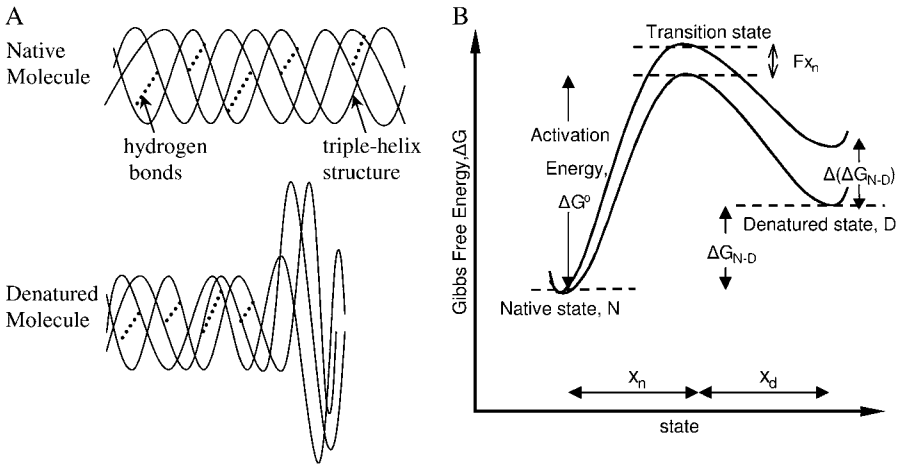

FIGURE 1 (*A*) Native and denatured states of the collagen molecule based on Harris and Humphrey (58). (*B*) Energy states of the collagen. There are two energy levels corresponding to the two states, with the native state being at the lower energy level. The activation Gibbs free energy is ΔG^{o}. Under tensile force, F, applied on the molecule, an extra term accounting for the mechanical work, Fx_n, contributes to the energy balance. x_n, distance between the native and the transition states; x_d, distance between the denatured and the transition states; $\Delta G_{N\text{-}D}$, energy of denaturation between the native and denatured states; $\Delta(\Delta G_{N\text{-}D})$, contribution of the mechanical work to the free energy of denaturation.

$$\frac{dN}{dt} = -kN, \tag{1}$$

where k is the rate constant, and t is the time. The rate constant at the stress-free state, k_o, is a function of the temperature, T, and is given by the Arrhenius equation:

$$k_o = A\exp\left(-\frac{\Delta E^{o}}{k_B T}\right), \tag{2}$$

where A is the (constant) frequency factor, k_B is Boltzmann's constant, and ΔE° is the activation energy. The rate constant can also be written using the transition state theory as (9,10)

$$k_o = \kappa\frac{k_B T}{h}\exp\left(\frac{\Delta S^{o}}{k_B}\right)\exp\left(-\frac{\Delta H^{o}}{k_B T}\right) = \kappa\frac{k_B T}{h}\exp\left(-\frac{\Delta G^{o}}{k_B T}\right), \tag{3}$$

where κ is the transmission coefficient, h is Planck's constant, and ΔS^{o}, ΔH^{o}, and ΔG^{o} are the activation entropy, enthalpy, and Gibbs free energy, respectively.

The tensile force applied on the molecule stabilizes the native state by increasing the Gibbs free energy by a factor of Fx_n (Fig. 1 *B*), where F is the applied tensile force and x_n is the distance between the native and the transition states (22,24–26). Therefore, when the collagen molecule is under tensile load, F, Eq. 3 can be written as

$$k = \kappa\frac{k_B T}{h}\exp\left(-\frac{\Delta G^{o} + Fx_n}{k_B T}\right) = k_o\exp\left(-\frac{Fx_n}{k_B T}\right). \tag{4}$$

Note that in Eq. 4, k_o can be calculated either from the Arrhenius equation (Eq. 2) or the transition state theory (Eq. 3).

In the model presented here, Eq. 4 is used to calculate the rate constant as a function of the tensile load on the collagen molecule and the isothermal temperature. The effects of other parameters (e.g., pH and electrolyte concentration (27)) on the rate of denaturation were not considered.

Studies (28,29) have shown that the response of the collagen molecule to tensile force is nonlinear. Thus, a phenomenological, exponential relationship was utilized to represent the force-elongation response of the collagen molecule in both the native and the denatured states (30–32),

$$F = \frac{E_m A_m}{B_m}(\exp(B_m\varepsilon_f) - 1), \tag{5}$$

where F is the force, A_m is the cross-sectional area of the molecule, ε_f is the Green strain given by $\varepsilon_f = 0.5(\lambda^2 - 1)$, where λ is the stretch ratio, and the constant B_m accounts for the nonlinearity of the response. For small displacements, i.e., $\lambda \to 1$, Eq. 5 reduces to the linear elastic model with modulus E_m. To account for the decrease in the molecule cross-sectional area in response to stretching, we assumed that the molecule was incompressible. Thus, the area A_m was computed using $A_m = A_o/\lambda$, where A_o is the cross-sectional area of the unstretched molecule.

The undeformed length of the collagen molecule in the native state was taken as 290 nm (33,34). It was assumed, based on shrinkage data for unloaded tissue (14,35), that the denatured collagen molecule shrank by 65% to a final length of 101.5 nm.

Fibril-level organization

The molecular organization and packing in collagen fibrils is complex (36–39). In our model, to represent the structure of the collagen fibril, a model similar to that used by Sasaki et al. (40) was employed. It was assumed that the neighboring collagen molecules are parallel to one another and are connected by cross-links in a staggered pattern forming molecular arrays (41). The molecular arrays are grouped together to form the fibril (Fig. 2 *A*). Under tension, the force, F_i, is transmitted through cross-links (in a staggered fashion), which was modeled using an in-series arrangement of molecules. The collagen fibril was modeled as an ensemble of collagen molecular arrays, parallel to one another, with the molecules connected at their end points by the cross-links (Fig. 2 *B*).

In tendons or ligaments, fibrils aggregate to form fibers, which in turn form fascicles (33). Given the complexity of the hierarchical structure of collagenous tissues, incorporation of all of the interactions among these individual units is considerably challenging. Therefore, as a first-level approximation, we assumed that the heat-induced response of the tissue is represented at the level of an individual fibril.

Based on Eq. 1, the incremental number of molecules expected to denature (ΔN) during a given short period of time Δt can be approximated by $N \times k\Delta t$. The probability, P, for a collagen molecule to denaturate when it is exposed to a hyperphysiological temperature is given by

$$P = k\Delta t \tag{6}$$

for small Δt, such that $k\Delta t \ll 1$.

As shown in Fig. 2 *B*, the total force F_{tot} applied to the fibril is the sum of forces, F_i, applied on the individual collagen molecular arrays:

$$F_{tot} = \sum F_i. \tag{7}$$

In the beginning of the solution algorithm ($t = 0$), the forces, F_i, of the parallel arrays were equal, enabling determination of the equilibrium

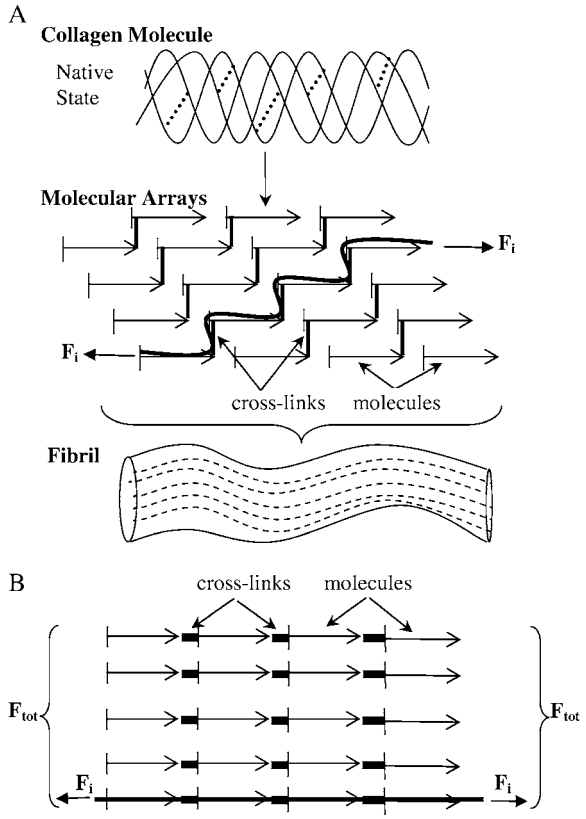

FIGURE 2 (*A*) Structure of the collagen fibril. The native state of the collagen molecule is shown. Molecules form a staggered pattern and are bonded together by cross-links. Molecular arrays are grouped together to form the fibril. Thick line shows the in-series arrangement of the molecules. (*B*) Model representation of the collagen fibril. Molecular arrays are aligned parallel to each other.

positions of the collagen molecules. The denaturation probability of each collagen molecule exposed to a temperature T and a tensile force F_i was determined, and a random number, r, between 0 and 1, was assigned to each molecule at the native state. If $r < P$, it was assumed that the native molecule had denaturated, its mechanical properties changed and its length decreased to those of the denatured state (42).

Since the denatured molecules were determined by a stochastic process, not all of the parallel molecular arrays had the same degree of denaturation (i.e., number of denatured molecules). Therefore, if the forces F_i applied to each array were the same, molecular arrays with more denatured molecules would be shorter than the arrays with fewer denatured molecules. The length of the molecular arrays, however, should be identical within the fibril, and the total force F_{tot} should be constant. Thus, at each time step in the Monte Carlo simulation, the forces F_i were redistributed among the parallel arrays to ensure a constant total force on the fibril and identical lengths for the molecular arrays. The solution algorithm can be summarized as follows: 1), A force, F_{tot} was applied to the collagen fibril. 2), Each molecule at the native state was tested for denaturation (i.e., their probability of denaturation was calculated). 3), The mechanical properties (i.e., the modulus) and the undeformed length were modified for the denatured molecules (i.e., those with a probability of denaturation larger than the denaturation probability at that temperature and load). 4), The forces, F_i, were recalculated to keep the total force constant (i.e., F_{tot} = constant) and to ensure identical lengths for the molecular arrays. 5), Steps 2–4 were repeated for the next time interval. A schematic of the algorithm is presented in Fig. 3.

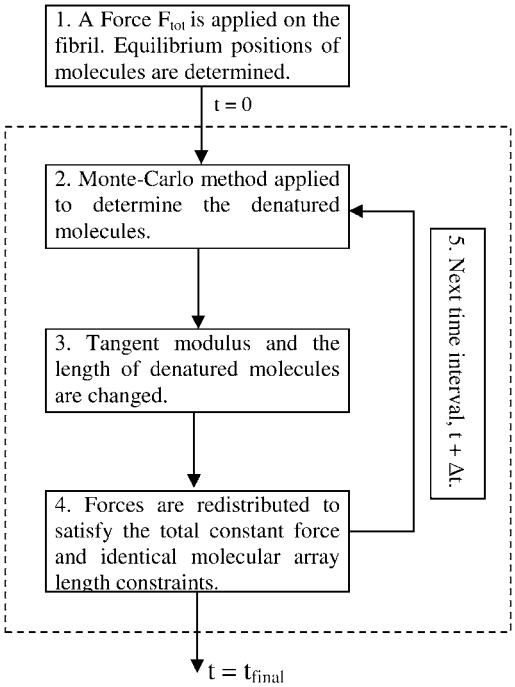

FIGURE 3 Schematic of the solution algorithm.

Model specification

The model predictions were compared to existing experimental data for New Zealand white rabbit patellar tendons previously reported by Aksan and McGrath (13). Those authors gave the constants A and ΔE^o for the Arrhenius equation as $A = 1.136\times10^{86}s^{-1}$ and $\Delta E^o = 5.623\times10^5 J/mol$. To calculate the rate constant under zero force, Eq. 2 was used, and since the activation energy was measured per mole (and not per molecule) the Boltzmann's constant, k_B, was replaced by the gas constant, R.

The experimental protocol included consecutive cycles of isothermal, isotonic shrinkage of the patellar tendon specimens by immersion in a water bath, followed by tensile testing to determine mechanical properties. The experiments were repeated for different sets of tensile loads and treatment temperatures. Four different load conditions were considered: 2.5, 5.0, 7.5, and 10.0 N and the treatment temperatures ranged from 66.34 to 72.25°C. During heating, the shrinkage of the tissue was measured as a function of the calculated thermal damage, Ω, given by the Arrhenius integral (43):

$$\Omega(\tau) = \int_0^\tau A \times e^{-(\Delta E^o/RT)} dt. \quad (8)$$

For an isothermal process, the above integral can be combined with Eq. 2 and written as

$$\Omega(t) = k_o t. \quad (9)$$

The model developed here was fitted to four randomly selected specimens reported in Aksan and McGrath (13), one for each load condition. The experimental conditions chosen are shown in Table 1.

The model contains 10 physical parameters, as listed in Table 2. Two of these parameters, A and ΔE^o, were determined independently in the previous study (13). The tangent modulus, E_n, and the diameter of the native collagen molecule were taken to be 4.0 GPa and 1.23 nm, respectively, based on reported values for undenatured systems (40,44,45). The constants B_n and B_d for the native and denatured states were determined by fitting Eq. 5 to the stress/strain response of the tendon before and after complete denaturation (A. Aksan, unpublished data) and found to be 1.0 and 0.35, respectively.

TABLE 1 Test conditions for the four specimens reported in the literature

Specimen number	Test load (N) (test stress (MPa))	Temperature average ± SD* (°C)
1	10.0 (0.725)	71.30 ± 1.39
3	7.5 (0.601)	70.72 ± 1.43
7	5.0 (0.312)	66.87 ± 1.38
8	2.5 (0.192)	66.34 ± 1.40

The four specimens in the table were evaluated by Aksan and McGrath (13).
*SD, the variation of the average temperature during the course of the experiment.

B_n and B_d were based on predenaturation or postdenaturation data, not on dynamic data, so they may be considered to have been determined independently with respect to the dynamics of denaturation. The length of the normal collagen molecule, L_n, is well established, and the shrinkage ratio for denatured tissues in the absence of load gives an excellent estimate of the rest length of the denatured collagen molecule, L_d. As mentioned earlier, the length of the native molecule was taken as 290 nm, and the length of the molecule in the denatured state was taken as 101.5 nm. The tangent modulus, E_d, of the denatured molecule was determined by regression to the experimental data and it was assumed that the cross-sectional area of the molecule did not change upon denaturation. The distance to the transition state, x_n, could be measured with single-molecule force spectroscopy, as has been done for ubiquitin (46). There are no reported values for collagen denaturation. The value of x_n in the model presented here was taken as constant. Calculations were performed by varying x_n from 0.2 to 1.7 nm (in the range reported for other proteins (47)) to explore how the model predictions depend on the choice of x_n. Thus, only the denatured molecule modulus, E_d, and the force, F_{tot}, were actually varied to ensure fit between the existing experimental data and the model predictions. The force, F_{tot}, was regressed for each experiment simulated, and the modulus, E_d, was determined to minimize the total prediction error over the four conditions studied.

TABLE 2 Model parameters

Model parameters	Value	Source
Arrhenius constant, A	1.135×10^{86} s^{-1}	Given in (13)
Activation energy, ΔE^o	5.63×10^5 J/mol	Given in (13)
Distance to the transient state, x_n (varied in this study)	0.2–1.7 nm	Estimated values based on (47)
Tangent modulus for native collagen, E_n	4.0 GPa	Reported values (40,44,45)
Tangent modulus for denatured collagen, E_d (depending on x_n)	132.6–17.7 MPa	Regressed to experiments (13)
Constant for native collagen, B_n	1.0	Based on (13)
Constant for denatured collagen, B_d	0.35	Based on (13)
Length of native molecule, L_n	290 nm	Given in (33,34)
Length of denatured molecule, L_d	101.5 nm	Based on (14,35)
Diameter of collagen molecule	1.23 nm	Given in (33,34)
Number of parallel molecular arrays	1000	Preliminary studies
Number of molecules per array	500	Preliminary studies

Typically, a collagen fibril consists of ~4000 molecular arrays (48). Our preliminary calculations gave similar results for fibrils made up of 1000–10,000 arrays, suggesting that a fibril model containing 1000 arrays is sufficient to capture the general features of the response. In a similar fashion, the effect of the number of molecules in an array on the predictions was examined. The results remained unchanged for arrays of >400 molecules. Thus, in the model, the number of molecules/array was set to 500.

RESULTS

In Figs. 4 and 5, the model predictions for tissue shrinkage as a function of thermal damage are presented and compared to the selected experiments. The shrinkage is defined as $1 - \Lambda$, where Λ is the ratio of the tissue length during heating to the length of the tissue before heating and is calculated as

$$1 - \Lambda = 1 - \frac{L}{L_o}, \tag{10}$$

where L is the current length of the tissue, and L_o is the tissue length before heating (at $t = 0$ in Fig. 3).

Fig. 4 shows the model predictions for $x_n = 0.2$ nm and Fig. 5 shows the model prediction for $x_n = 1.7$ nm. The shrinkage versus thermal damage curves for the other values of x_n employed in this study (not shown) gave similar goodness of fit. The model predicts the heat-induced shrinkage of the tissue for the whole range of tensile loads and temperatures tested. The R^2 value is also given in the captions of the plots to describe the predictive power of the model. The model fit to the experimental data is very good for both values of x_n, resulting in R^2 values of 0.95 or higher (the closer R^2 is to 1, the better the model). The forces applied on each molecular array (F_i) for the four experimental cases and for $x_n = 0.2$ nm

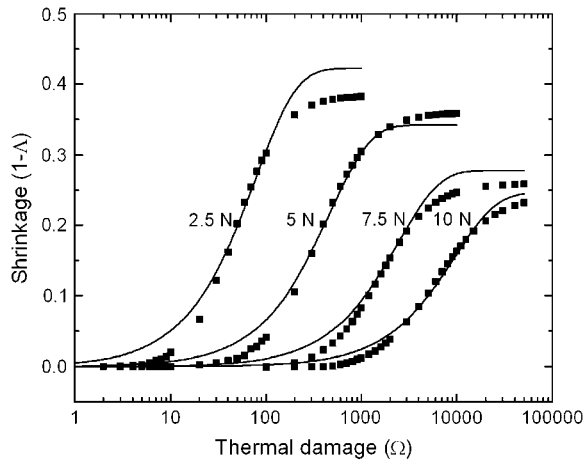

FIGURE 4 Shrinkage versus thermal damage for computed (*solid line*) and experimental (*squares*) results. The value of x_n is 0.2 nm, and the modulus E_d was calculated as 132.6 MPa. Specimen 1, test load 10 N, calculated force/molecular array 218 pN, $R^2 = 0.987$. Specimen 3, test load 7.5 N, calculated force/molecular array 185 pN, $R^2 = 0.967$. Specimen 7, test load 5 N, calculated force/molecular array 144 pN, $R^2 = 0.989$. Specimen 8, test load 2.5 N, calculated force/molecular array 102 pN, $R^2 = 0.967$.

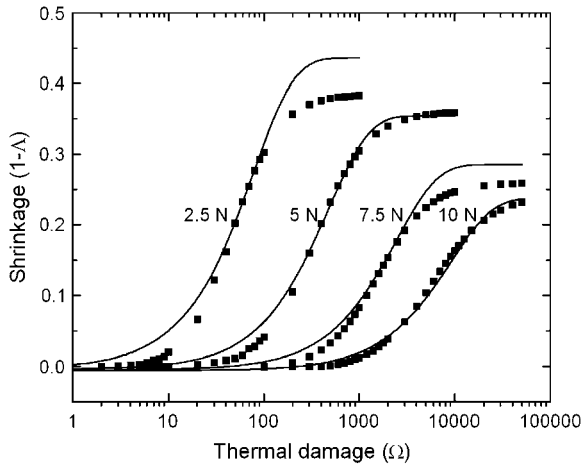

FIGURE 5 Shrinkage versus thermal damage for computed (*solid line*) and experimental (*squares*) results. The value of x_n is 1.7 nm, and the modulus E_d was calculated as 17.7 MPa. Specimen 1, test load 10 N, calculated force/molecular array 26 pN, $R^2 = 0.994$. Specimen 3, test load 7.5 N, calculated force/molecular array 22 pN, $R^2 = 0.990$. Specimen 7, test load 5 N, calculated force/molecular array 17 pN, $R^2 = 0.993$. Specimen 8, test load 2.5 N, calculated force/molecular array 12 pN, $R^2 = 0.950$.

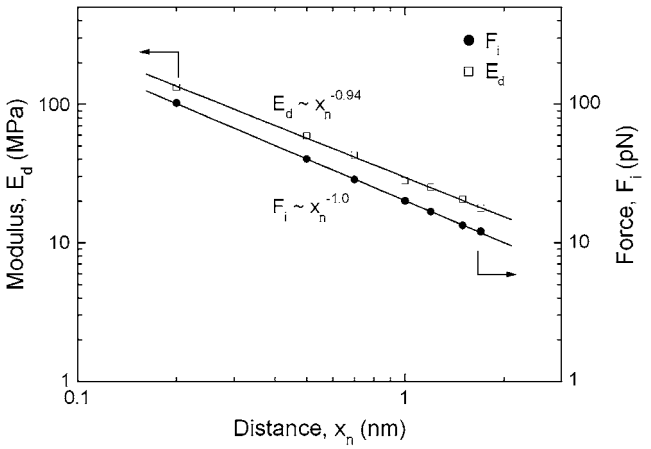

FIGURE 6 Variation of calculated E_d and F_i (for specimen 8) with x_n.

and $x_n = 1.7$ nm are shown in Table 3. We see that increasing x_n decreases the force, F_i. Note that for the Results and Discussion sections, the values of F_i presented are at time $t = 0$, where all molecular arrays carry the same force.

Fig. 6 depicts the dependence of E_d and F_i (for specimen 8) on x_n. Increasing x_n decreases the calculated force F_i and the modulus of the denatured molecule, E_d. The decrease in F_i results from the kinetics of denaturation for k to remain unchanged (Eq. 4), whereas the decrease in E_d is subsequent to the decrease in F_i, so that the same levels of shrinkage are achieved (Eq. 5). The two curves can be fitted by the power law functions $\log F_i = 1.3 - \log x_n$ and $\log E_d = 1.47 - 0.94 \log x_n$.

So far, we have shown that the choice of x_n only affects the fitting parameter, E_d, and not the model predictions. For the rest of the simulations, the value of x_n was kept constant at 1.7 nm. Simulations were also performed to further address the effect of temperature and force on thermal denaturation kinetics. For the first series of simulations, the force (F_i) was kept constant at 15 pN and the temperature was varied from 64 to 72°C. The change of the degree of denaturation with time was recorded and the results are presented in Fig. 7 *A*. The degree of denaturation is given as the ratio of the denatured molecules in the fibril over the total number of molecules. In Fig. 7 *B*, the temperature was kept constant at 66°C and the

TABLE 3 Previously reported test loads and forces applied to molecular arrays as calculated with the model

Specimen number	Test load (N)	Force/array, F_i (pN) $x_n = 0.2$ nm	Force/array, F_i (pN) $x_n = 1.7$ nm
1	10.0	218.0	26.0
3	7.5	185.0	22.0
7	5.0	144.0	17.0
8	2.5	102.0	12.0

The test loads reported were from Aksan and McGrath (13).

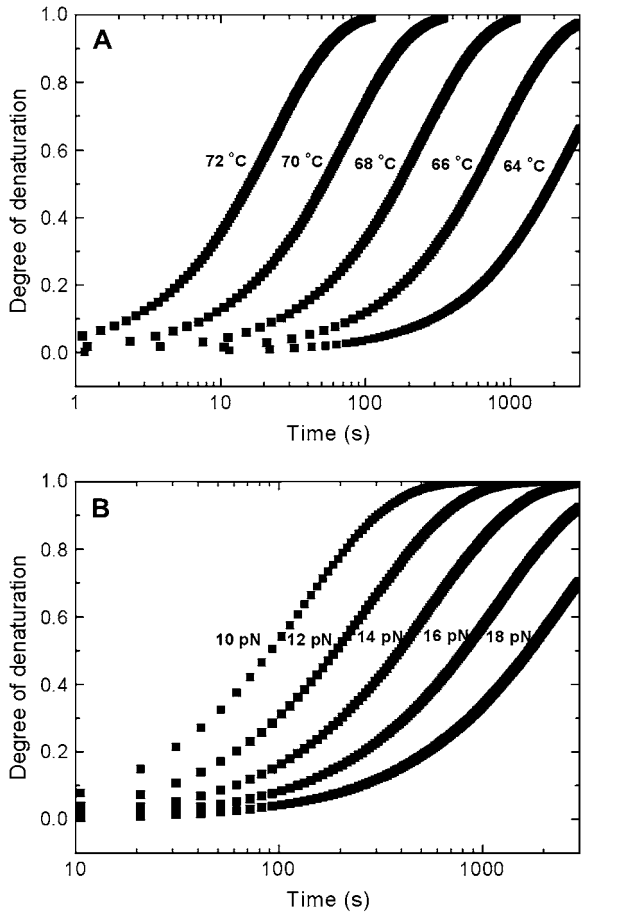

FIGURE 7 Predicted denaturation kinetics for (*A*) $F_i = 15$ pN while the temperature is increased from 64 to 72°C, and (*B*) $T = 66$°C while the force varies from 10 to 18 pN. The value of x_n is 1.7 nm.

force was varied from 10 to 18 pN. It was observed that the effects of increasing the temperature and decreasing the load were the same; both increased the rate of denaturation. This was consistent with experimental observations.

Experimental observations in one-dimensional tissues have also revealed a ''time-temperature-load equivalency.'' If the denaturation time is scaled over a characteristic value, the denaturation curves for different sets of temperatures and loads fall on the same master curve (13,14). Taking the time that corresponds to 50% denaturation as a characteristic time, and plotting the denaturation curves of Fig. 7, *A* and *B*, together, we observe that such a relationship between time, temperature, and load is also predicted by the model. The predicted master curve and the experimental curves for the four specimens are plotted in Fig. 8. For the experiments, the degree of denaturation was estimated as $(1-\Lambda)/(1-\Lambda)_{\max}$.

In Aksan and McGrath (13), the changes in the mechanical properties of the tissue were also measured, and it was shown that the decrease in the tangent modulus with shrinkage of the tendon followed the same (master) curve, independent of the treatment temperature and load. To test the ability of the presented methodology to capture the heat-induced alterations in the mechanical behavior of the tissue, the tangent modulus of the fibril was calculated for the four studied cases. As stated in Fung (33), the tangent modulus of the fibril cannot be derived from multiple moduli of the molecules. Therefore, for the calculation of the fibril's tangent modulus a method similar to that used in the experiments was employed. The simulations shown in Fig. 5 were repeated, but were terminated at different degrees of thermal damage, and then the whole fibril was stretched to a final Green strain ranging from 40% (native fibril) to 200% (totally denatured fibril), and the stress/strain response of the fibril was recorded. From the slope of the linear part of the curves, the tangent modulus was calculated. To measure the strain, the initial length of the fibril was taken to be the fibril length before stretching of the fiber; in accordance with the experimental measurements. Results were given as the decrease in the tangent modulus E/E_o, where E is the tangent modulus of the collagen fibril and E_o is the tangent modulus of the native collagen fibril, versus the shrinkage of the tissue. Fig. 9 depicts the computed decrease in the tangent modulus and the master curve measured experimentally in Aksan and McGrath (13).

DISCUSSION

In this work, we developed a structure-based model for collagenous tissue thermomechanics that incorporated the tissue molecular and structural architecture to predict the gross tissue response. Despite its simplicity, the model could simulate unidirectional collagenous tissue behavior in the range of tensile loads and temperatures previously studied. The model also predicted the experimentally observed time-temperature-load equivalency, and the rate of degradation of the mechanical properties of the tissues during denaturation.

A crucial parameter used in the method described here is the distance between the native and transition states, x_n, which appears in Eq. 4. The value of x_n for the thermal denaturation of the collagen molecule is not known but it could be measured experimentally, as has been done for the unfolding of other proteins (46). We decided to vary x_n from 0.2 to 1.7 nm, in the range reported for other proteins (47), and we showed that the model could predict the experimental tissue response for any value of x_n. Any change in the value of x_n resulted in changing the force F_i so that the rate constant given by Eq. 4 remained the same. The change in force, in turn, resulted in decrease of E_d so that the same levels of shrinkage were reached (Eq. 5). Therefore, in our analysis, collagen denaturation can be seen as a process governed by two dimensionless quantities, an energy parameter Fx_n/k_BT, and a force parameter F/E_dA_d. As long as these two parameters remain the same,

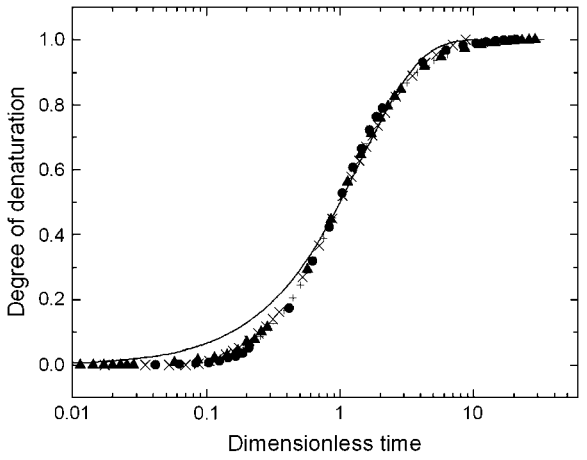

FIGURE 8 Master curve (*solid line*) showing the predicted time-temperature-load equivalency. The experimental measurements are also shown: specimen 1 (×), specimen 3 (+), specimen 7 (▲), and specimen 8 (●). Dimensionless time is the time divided by the time at 50% denaturation.

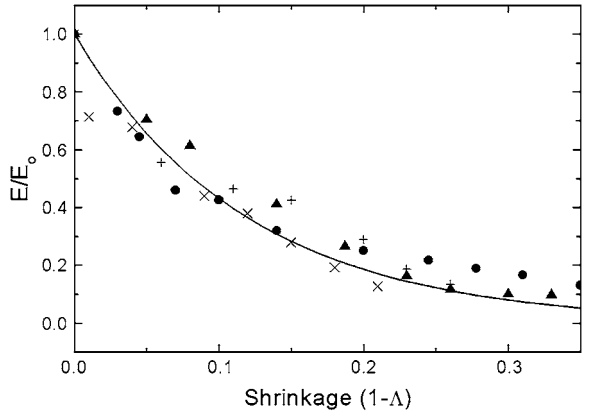

FIGURE 9 Decrease in the normalized tangent modulus of the fibril, E/E_o, with shrinkage $(1-\Lambda)$ for the experimental (*solid line*) and the computed results for the four studied conditions: specimen 1 (×), specimen 3 (+), specimen 7 (▲), and specimen 8 (●). The value of x_n is 1.7 nm.

the predicted response of the tissue will be the same, only deviating due to the fluctuations arising from the stochastic nature of the model. The value of x_n, however, can vary considerably for different systems, and for this reason the value of x_n for the collagen molecule must be experimentally determined to achieve more accurate predictions.

Another, possibly useful, prediction of the model is based on the fact that more than one pair of temperatures and forces (T, F) can give the same value of the rate constant, k. A relationship between two different such pairs can be derived from Eqs. 2 and 4,

$$\frac{T_2}{T_1} = \frac{\Delta E^o + F_2 x_n}{\Delta E^o + F_1 x_n}. \quad (11)$$

According to the model, Eq. (11) describes all the pairs of (T, F) for which the denaturation response of the tissue, expressed as degree of denaturation versus time, will be the same. This is of importance if we consider the fact that, so far, the selection of temperatures and loads with which researchers experiment is based on empirical observation and not on an established guideline. Therefore, the model could be possibly used as such a guide. However, further experimental analysis is required to determine the range of validity of these predictions.

The predicted force F_i was in the range 12–218 pN, depending on the value of x_n used and the specimen number (see Table 3). Experimental studies of the mechanical properties of single collagen molecules report force values that fall into the same range (28,29). Another consideration is that even though the load on the tendon increased by a factor of 4 (from 2.5 to 10 N), the force on the molecular array changed by a factor of ~2.15. This discrepancy may be due to the fact that the model ignores interactions among fibrils and among higher-order units that comprise the tendon (fibers and fascicles). Additional factors are the presence of components other than collagen, like proteoglycans and the interstitial fluid contributing to the overall mechanical response of the tissue. In addition to that, the model incorporates only tensile forces applied to the molecules. However, it is also possible that shear forces develop (49) and contribute to the interactions between molecular arrays. Furthermore, the assumption of collagen molecule incompressibility is a simplification, and also, as the diameter of the molecule decreases, the forces due to water hydration increase considerably (50,51). This could affect the force-elongation relationship (Eq. 5). Table 3 shows that every time the load on the tendon is doubled, the force on the molecular array increases by a factor of 1.2 to 1.4, which implies that the increase in the microscopic force follows the same trend as the increase in the macroscopic load.

The tangent modulus of the denatured molecule was found to range from 132.6 to 17.7 MPa (depending on the choice of x_n), much lower than the modulus of the native molecule (4 GPa), which is in agreement with the experimental observations (13,20,52). Also, note that when calculating E_d, it was assumed that the cross-sectional area of the molecule did not change with denaturation. There is experimental evidence, however, showing that the denatured fiber is thicker than the native (53), and thus, the molecule must be thicker in the denatured state. Therefore, the tangent modulus might be even lower.

The two-state model has been used for describing the mechanical unfolding of proteins in many studies (22,23,54). For the thermal transition of collagen, however, there is evidence that the two-state approximation might not be ideal (55), and even that the mechanism of collagen molecule unfolding might not be the same as with other protein molecules (e.g., fibronectin) (56). This study has shown that irrespective of the intermediate states, the two-state model might be sufficient to perform thermomechanical analyses that require information on the kinetics of thermal damage.

The mathematical model presented is based on the idea that tensile forces stabilize the collagen molecule by increasing the Gibbs free energy of the system. This can be explained by the fact that the applied force decreases the possible number of configurations that the collagen molecule can take and consequently decreases the conformational entropy of the system. This is in agreement with previously reported results by Miles and Ghelashvili (57).

We have modeled the thermomechanical response of collagenous tissues as a stochastic process, where initially all of the collagen molecules have the same probability of denaturation. During thermal denaturation, therefore, the degree of denaturation in different molecular arrays (i.e., the number of denatured molecules in each array) varies. Arrays with a higher degree of denaturation (higher number of denatured molecules) carry higher loads as they experience larger strains. Therefore, native molecules in the arrays with a higher degree of denaturation have decreased probability of denaturation. This process is in agreement with other studies (19,53), in which the authors examined the effect of the interactions among the constituents on the thermal damage of tissues.

Of great importance is the incorporation of this kinetic approach into existing biomechanical models. In general, there is a lack of structural thermomechanical models that predict the various stages of thermal damage accumulation in soft tissues while providing a correlation between thermal damage and the changes in the mechanical properties of the tissue. The biomechanical models now being used examine collagenous tissues as matrices of a very high number of interacting or noninteracting fibrils (31,32). The observed time-temperature-load equivalency, however, simplifies the solution algorithm considerably, since the degree of denaturation (as well as its tissue level outcome) can be calculated by using a single parameter, the characteristic time. If the dependence of the characteristic time on temperature and load was explicitly known, the shrinkage and the degradation of the mechanical properties of the collagen fibrils at any time, temperature, and load would be known. Experimentally

derived equations that relate the characteristic time to load and temperature changes for specific tissues have been reported (14). A mathematical framework that would provide accurate predictions of the characteristic time for any set of temperatures and loads and for any tissue type is therefore required.

We thank David Morse and David Odde for fruitful discussions, and the anonymous reviewers for their insightful comments.

This work was supported by the National Institutes of Health (R01 EB005813-01). T.S. was also supported by a Doctoral Dissertation Fellowship from the University of Minnesota. Simulations were made possible by a Resource Grant from the University of Minnesota Supercomputer Institute and TeraGrid.

REFERENCES

1. Miniaci, A., and J. McBirnie. 2003. Thermal capsular shrinkage for treatment of multidirectional instability of the shoulder. *J. Bone Joint Surg. Am.* 85-A:2283–2287.
2. Wallace, A. L., R. M. Hollinshead, and C. B. Frank. 2001. Electrothermal shrinkage reduces laxity but alters creep behavior in a lapine ligament model. *J. Shoulder Elbow Surg.* 10:1–6.
3. Lubowitz, J. H. 2005. Thermal modification of the lax anterior cruciate ligament using radiofrequency: efficacy or catastrophe? *Knee Surg. Sports Traumatol. Arthrosc.* 13:432–436.
4. Brinkmann, R., B. Radt, C. Flamm, J. Kampmeier, N. Koop, and R. Birngruber. 2000. Influence of temperature and time on thermally induced forces in corneal collagen and the effect on laser thermokeratoplasty. *J. Cataract Refract. Surg.* 26:744–754.
5. Kuo, T., M. T. Speyer, W. R. Ries, and L. Reinisch. 1998. Collagen thermal damage and collagen synthesis after cutaneous laser resurfacing. *Lasers Surg. Med.* 23:66–71.
6. Wright, N. T., and J. D. Humphrey. 2002. Denaturation of collagen via heating: an irreversible rate process. *Annu. Rev. Biomed. Eng.* 4:109–128.
7. Arnoczky, S. P., and A. Aksan. 2000. Thermal modification of connective tissues: basic science considerations and clinical implications. *J. Am. Acad. Orthop. Surg.* 8:305–313.
8. Wallace, A. L., R. M. Hollinshead, and C. B. Frank. 2000. The scientific basis of thermal capsular shrinkage. *J. Shoulder Elbow Surg.* 9:354–360.
9. Miles, C. A. 1993. Kinetics of collagen denaturation in mammalian lens capsules studied by differential scanning calorimetry. *Int. J. Biol. Macromol.* 15:265–271.
10. Miles, C. A., T. V. Burjanadze, and A. J. Bailey. 1995. The kinetics of the thermal denaturation of collagen in unrestrained rat tail tendon determined by differential scanning calorimetry. *J. Mol. Biol.* 245:437–446.
11. Pearce, J. A., and S. Thomsen. 1993. Kinetic models of laser-tissue fusion processes. *Biomed. Sci. Instrum.* 29:355–360.
12. Bischof, J. C., and X. He. 2006. Thermal stability of proteins. *Ann. N. Y. Acad. Sci.* 1066:12–33.
13. Aksan, A., and J. J. McGrath. 2003. Thermomechanical analysis of soft-tissue thermotherapy. *J. Biomech. Eng.* 125:700–708.
14. Chen, S. S., N. T. Wright, and J. D. Humphrey. 1998. Heat-induced changes in the mechanics of a collagenous tissue: isothermal, isotonic shrinkage. *J. Biomech. Eng.* 120:382–388.
15. Harris, J. L., P. B. Wells, and J. D. Humphrey. 2003. Altered mechanical behavior of epicardium due to isothermal heating under biaxial isotonic loads. *J. Biomech. Eng.* 125:381–388.
16. Thomsen, S., J. A. Pearce, and W. F. Cheong. 1989. Changes in birefringence as markers of thermal damage in tissues. *IEEE Trans. Biomed. Eng.* 36:1174–1179.
17. Viidik, A. 1972. Aging of collagen in complex tissues. A micromethodological study of the thermal reaction. *Experientia.* 28:641–642.
18. Chen, S. S., N. T. Wright, and J. D. Humphrey. 1998. Phenomenological evolution equations for heat-induced shrinkage of a collagenous tissue. *IEEE Trans. Biomed. Eng.* 45:1234–1240.
19. Danielsen, C. C. 1981. Thermal stability of reconstituted collagen fibrils. Shrinkage characteristics upon in vitro maturation. *Mech. Ageing Dev.* 15:269–278.
20. Wall, M. S., X. H. Deng, P. A. Torzilli, S. B. Doty, S. J. O'Brien, and R. F. Warren. 1999. Thermal modification of collagen. *J. Shoulder Elbow Surg.* 8:339–344.
21. Tao, L., J. D. Humphrey, and K. R. Rajagopal. 2001. A mixture theory for heat-induced alterations in hydration and mechanical properties in soft tissues. *Int. J. Eng. Sci.* 39:1535–1556.
22. Rounsevell, R., J. R. Forman, and J. Clarke. 2004. Atomic force microscopy: mechanical unfolding of proteins. *Methods.* 34:100–111.
23. Karcher, H., S. E. Lee, M. R. Kaazempur-Mofrad, and R. D. Kamm. 2006. A coarse-grained model for force-induced protein deformation and kinetics. *Biophys. J.* 90:2686–2697.
24. Bell, G. I. 1978. Models for the specific adhesion of cells to cells. *Science.* 200:618–627.
25. Evans, E., and K. Ritchie. 1997. Dynamic strength of molecular adhesion bonds. *Biophys. J.* 72:1541–1555.
26. Howard, J. 2001. Mechanics of Motor Proteins and the Cytoskeleton. Sinauer Press, Sunderland, MA.
27. Lennox, F. G. 1949. Shrinkage of collagen. *Biochim. Biophys. Acta.* 3: 170–187.
28. Sun, Y. L., Z. P. Luo, A. Fertala, and K. N. An. 2002. Direct quantification of the flexibility of type I collagen monomer. *Biochem. Biophys. Res. Commun.* 295:382–386.
29. Bozec, L., and M. Horton. 2005. Topography and mechanical properties of single molecules of type I collagen using atomic force microscopy. *Biophys. J.* 88:4223–4231.
30. Billiar, K. L., and M. S. Sacks. 2000. Biaxial mechanical properties of the native and glutaraldehyde-treated aortic valve cusp: Part II—A structural constitutive model. *J. Biomech. Eng.* 122:327–335.
31. Stylianopoulos, T., and V. H. Barocas. 2007. Volume-averaging theory for the study of the mechanics of collagen networks. *Comput. Methods Appl. Mech. Eng.* 196:2981–2990.
32. Stylianopoulos, T., and V. H. Barocas. 2007. Multiscale, structure-based modeling for the elastic mechanical behavior of arterial walls. *J. Biomech. Eng.* 129:611–618.
33. Fung, Y. C. 1993. Biomechanics: Mechanical Properties of Living Tissues. Springer-Verlag, New York.
34. Humphrey, J. D. 2002. Cardiovascular Solid Mechanics, Cells, Tissues and Organs. Springer-Verlag, New York.
35. Chen, S. S., N. T. Wright, and J. D. Humphrey. 1997. Heat-induced changes in the mechanics of a collagenous tissue: isothermal free shrinkage. *J. Biomech. Eng.* 119:372–378.
36. Fraser, R. D., T. P. MacRae, A. Miller, and E. Suzuki. 1983. Molecular conformation and packing in collagen fibrils. *J. Mol. Biol.* 167:497–521.
37. Wess, T. J., A. P. Hammersley, L. Wess, and A. Miller. 1998. Molecular packing of type I collagen in tendon. *J. Mol. Biol.* 275:255–267.
38. Cowin, S. C. 2000. How is a tissue built? *J. Biomech. Eng.* 122:553–569.
39. Israelowitz, M., S. W. Rizvi, J. Kramer, and H. P. von Schroeder. 2005. Computational modeling of type I collagen fibers to determine the extracellular matrix structure of connective tissues. *Protein Eng. Des. Sel.* 18:329–335.
40. Sasaki, N., and S. Odajima. 1996. Stress-strain curve and Young's modulus of a collagen molecule as determined by the X-ray diffraction technique. *J. Biomech.* 29:655–658.
41. Lees, S. 1985. Water content in type I collagen tissues calculated from the generalized packing model. *Int. J. Biol. Macromol.* 8:66–72.

42. Metropolis, N., A. W. Rosenbluth, M. N. Rosenbluth, and A. H. Teller. 1953. Equation of state calculations by fast computing machines. *J. Chem. Phys.* 21:1087–1092.

43. Henriques, F. C. J. 1947. Studies of thermal injury: V. The predictability and the significance of thermally induced rate processes leading to irreversible epidermal injury. *Arch. Pathol.* 43:489–502.

44. Lorenzo, A. C., and E. R. Caffarena. 2005. Elastic properties, Young's modulus determination and structural stability of the tropocollagen molecule: a computational study by steered molecular dynamics. *J. Biomech.* 38:1527–1533.

45. Silver, F. H., I. Horvath, and D. J. Foran. 2001. Viscoelasticity of the vessel wall: the role of collagen and elastic fibers. *Crit. Rev. Biomed. Eng.* 29:279–301.

46. Brujic, J., R. I. Hermans, K. A. Walther, and J. M. Fernandez. 2006. Single-molecule force spectroscopy reveals signatures of glassy dynamics in the energy landscape of ubiquitin. *Nature Physics.* 2:282–286.

47. Raible, M., M. Evstigneev, F. W. Bartels, R. Eckel, M. Nguyen-Duong, R. Merkel, R. Ros, D. Anselmetti, and P. Reimann. 2006. Theoretical analysis of single-molecule force spectroscopy experiments: heterogeneity of chemical bonds. *Biophys. J.* 90:3851–3864.

48. Hulmes, D. J., T. J. Wess, D. J. Prockop, and P. Fratzl. 1995. Radial packing, order, and disorder in collagen fibrils. *Biophys. J.* 68:1661–1670.

49. Buehler, M. J. 2006. Nature designs tough collagen: explaining the nanostructure of collagen fibrils. *Proc. Natl. Acad. Sci. USA.* 103: 12285–12290.

50. Leikin, S., D. C. Rau, and V. A. Parsegian. 1994. Direct measurement of forces between self-assembled proteins: temperature-dependent exponential forces between collagen triple helices. *Proc. Natl. Acad. Sci. USA.* 91:276–280.

51. Kuznetsova, N., D. C. Rau, V. A. Parsegian, and S. Leikin. 1997. Solvent hydrogen-bond network in protein self-assembly: solvation of collagen triple helices in nonaqueous solvents. *Biophys. J.* 72:353–362.

52. Chen, S. S., and J. D. Humphrey. 1998. Heat-induced changes in the mechanics of a collagenous tissue: pseudoelastic behavior at 37°C. *J. Biomech.* 31:211–216.

53. Wells, P. B., S. Thomsen, M. A. Jones, S. Baek, and J. D. Humphrey. 2005. Histological evidence for the role of mechanical stress in modulating thermal denaturation of collagen. *Biomech. Model. Mechanobiol.* 4:201–210.

54. West, D. K., P. D. Olmsted, and E. Paci. 2006. Mechanical unfolding revisited through a simple but realistic model. *J. Chem. Phys.* 124:1–8.

55. Persikov, A. V., Y. Xu, and B. Brodsky. 2004. Equilibrium thermal transitions of collagen model peptides. *Protein Sci.* 13:893–902.

56. Leikina, E., M. V. Mertts, N. Kuznetsova, and S. Leikin. 2002. Type I collagen is thermally unstable at body temperature. *Proc. Natl. Acad. Sci. USA.* 99:1314–1318.

57. Miles, C. A., and M. Ghelashvili. 1999. Polymer-in-a-box mechanism for the thermal stabilization of collagen molecules in fibers. *Biophys. J.* 76:3243–3252.

58. Harris, J. L., and J. D. Humphrey. 2004. Kinetics of thermal damage to a collagenous membrane under biaxial isotonic loading. *IEEE Trans. Biomed. Eng.* 51:371–379.